Guiding the Patterned Growth of Neuronal Axons and Dendrites Using Anisotropic Micropillar Scaffolds

Shengying Fan, Lei Qi, Jiawen Li,* Deng Pan, Yiyuan Zhang, Rui Li, Cong Zhang, Dong Wu, Pakming Lau, Yanlei Hu, Guoqiang Bi,* Weiping Ding,* and Jiaru Chu

The patterning of axonal and dendritic growth is an important topic in neural tissue engineering and critical for generating directed neuronal networks in vitro. Evidence shows that artificial micro/nanotopography can better mimic the environment for neuronal growth in vivo. However, the potential mechanisms by which neurons interact with true three dimensional (3D) topographical cues and form directional networks are unclear. Herein, 3D micropillar scaffolds are designed to guide the growth of neural stem cells and hippocampal neurons in vitro. Discontinuous and anisotropic micropillars are fabricated by femtosecond direct laser writing to form patterned scaffolds with various spacings and heights, which are found to affect the branching and orientation of axons and dendrites. Interestingly, axons and dendrites tend to grow on an array of 3D micropillar scaffolds of the same height and form functionally connected neuronal networks, as reflected by synchronous neuronal activity visualized by calcium imaging. This method may represent a promising tool for studying neuron behavior and directed neuronal networks in a 3D environment.

S. Fan, Prof. W. Ding
Center for Biomedical Engineering
Department of Electronic Science and Technology
University of Science and Technology of China
Hefei 230026, China
E-mail: wpdings@ustc.edu.cn
Dr. L. Qi, Prof. P. Lau, Prof. G. Bi
CAS Key Laboratory of Brain Function and Disease
School of Life Sciences
Division of Life Sciences and Medicine
University of Science and Technology of China
Hefei 230026, China
E-mail: gqbi@ustc.edu.cn
Dr. L. Qi, Prof. P. Lau, Prof. G. Bi
Hefei National Laboratory for Physical Sciences at the Microscale
University of Science and Technology of China
Hefei 230026, China
Prof. J. Li, D. Pan, Y. Zhang, R. Li, C. Zhang, Prof. D. Wu, Prof. Y. Hu, Prof. J. Chu
Key Laboratory of Precision Scientific Instrumentation of Anhui Higher Education Institutes
CAS Key Laboratory of Mechanical Behavior and Design of Materials
Department of Precision Machinery and Precision Instrumentation
University of Science and Technology of China
Hefei 230026, China
E-mail: jwl@ustc.edu.cn

The ORCID identification number(s) for the author(s) of this article can be found under https://doi.org/10.1002/adhm.202100094

1. Introduction

Neurological dysfunction caused by aging, trauma or neurodegeneration can lead to severe disability, which is a major concern in an aging society.[1] The regeneration and repair of nerve tissue require many important cells and extracellular components, which interact in many ways. As a scaffold for cell growth, extracellular substrates can provide signals that affect cell behavior and facilitate neural function, although the goal of guiding the directional growth of cells during development is a challenge.[2] Such scaffolds are especially important in guiding the directional growth and branching of neurons to form directional neuronal networks between adjacent neurons.[3] Neurons are functional units of nerve tissue that are responsible for transmitting information to the surroundings through electrical and chemical signals. Unlike cells in other tissues, such as epithelia, myocardial cells, skeletal muscle cells, etc., which present with simple shapes, neural tissues exhibit complex three dimensional (3D) topographic features, including a wide range of morphologies and scales.[4] Neuron shape exhibits a highly polarized pattern that consists of two types of neurite extensions from the cell body, namely, dendrites, and axons.

Increasing evidence shows that complex extracellular environments, including biochemical signals,[5] extracellular matrix components,[6] physical parameters (e.g., terrain and stiffness),[7] and surrounding cell compositions, affect cell morphology, adhesion, proliferation, and differentiation; axon/dendrite orientation, branching and length; and even the life process of cells. Among the complex extracellular environments, the influence of artificial micro- or nanotopographic features on the morphology and function of neurons has been widely studied because such features can better mimic the 3D environment in which cells grow in the body.[8] Topologies can generally be classified into continuous topologies and discontinuous topologies based on different geometric features.[9] The typical morphologies of continuous topologies include grooved and fibrous substrates, whereas that of discontinuous geometries include periodically or arbitrarily distributed micropillars or microposts.[10,11] Topologies can be further classified into isotropic and anisotropic topologies based on the directionality of topographic features. Isotropic topologies provide cues in random direction axes,

**ADVANCED
SCIENCE NEWS**

www.advancedsciencenews.com

**ADVANCED
HEALTHCARE
MATERIALS**

www.advhealthmat.de

while anisotropic topologies can guide cell growth in a directed direction.[12] In addition, anisotropic topographies can support stronger neurite guidance than isotropic topographies of the same scale.

Interestingly, discontinuous anisotropic topographies show strong topography-induced neuron orientation. C. Simitzi et al. studied the relationship between neurite length and anisotropic micropillar topography and found that hippocampal neurons preferred interrupted cues rather than continuous cues for guidance.[13] Repić et al. studied the effect of micropillars with different widths and spacings on the length and number of adult neonatal dorsal root ganglion (DRG) neurons and proposed that micropillars induced specific directional growth of DRG neurites.[9] These previous works focused on 2D micropillar scaffolds to study the interaction between the number or length of neurons and the spacing or width of scaffolds. The effect of scaffold spacing on branches and orientations of neurons has not been studied systematically. However, directed neuronal networks depend on controlled axon and dendrite branching and synapse formation.[14,15] During the development of nerve cells, the establishment of complex brain circuits requires the control of the branches and positions of each neuron. Moreover, cells live in a 3D environment in vivo; therefore, the 3D neuronal network model provides broad prospects for understanding the development, function, and disease pathology of the brain. However, proper development and function of the 3D neuronal network depends on the interaction of cells and the environment, and the influence of 3D micropillar scaffolds on guiding neuronal cell growth has not yet been investigated. Advanced micro/nanofabrication technologies, including photolithography, chemical vapor deposition, and nanoimprinting, have been used for customized microstructures and specific topographies.[16,17] However, it is still difficult to fabricate 3D micropillar scaffolds with different heights and submicron resolutions by these methods.

Femtosecond direct laser writing (fs-DLW) is a promising method with the advantages of flexibility, high resolution and true 3D processing, and it has been widely used in the fields of biological diagnosis, medical components, and 3D vascular scaffolds.[18,19] Here, we employ fs-DLW to fabricate 3D micropillar scaffolds of various spacings and heights by simply inputting the computer-aided design 3D model. The 3D scaffolds can be prepared in a short time without additional processes, which provides a flexible strategy to fabricate arbitrary 3D extracellular scaffolds. Micropillar scaffolds of various heights are first designed to guide directional growth of axons and dendrites to form neuronal networks. In addition, two representative cell lines, namely, neurons differentiated by neural stem cells (NSCs) and hippocampal neurons, were selected to reveal the interaction between scaffolds and cells. NSCs can produce serial passages, therefore, the experiments have good stability and repeatability. The guiding effects of cell scaffolds on neurons are systematically investigated on predesigned discontinuous, anisotropic, micropillar scaffolds of various spacings and heights. Moreover, a novel 3D microring that consists of micropillars with different heights guides the directional growth of hippocampal neurons to form autaptic neurons for the first time. Finally, the Ca²⁺ activity of the organized neuronal network on micropillar scaffolds is synchronized, which verifies that neurons can form normal neuronal networks. This work has guiding significance for studying the growth, orientation and branching of neuron cells in a 3D extracellular environment,[20] which has promising applications in the field of synaptic signaling, nerve repair and neural tissue engineering.[21,22]

2. Results and Discussion

2.1. Directional Growth of Neurons Guided by Programmable One-Step Fabrication of Anisotropic 3D Micropillar Scaffolds

Discontinuous and anisotropic 3D micropillar scaffolds with different spacings and heights are fabricated by one-step fs-DLW, which is schematically shown in **Figure 1**a. Anisotropic micropillar scaffolds with the same height and different spacings are fabricated to guide the growth of neurons. The proximal distance of the micropillar scaffold is 3 μm on one axis (the "proximal axis"), and the distal distance of the other axis (the "distal axis") is 3, 6, 9, and 12 μm, with a height of 6 μm and diameter of 1 μm (Figure 1b–e). In addition, programmable patterned anisotropic 3D micropillar scaffolds with the same spacing and different heights are fabricated. The distances of the 3D micropillars on the proximal axis and the distal axis are the same (3 μm), while the heights of the micropillars are 2, 4, and 6 μm (Figure 1f). In addition, micropillars of various heights (3, 6, and 9 μm) are patterned to form novel 3D microrings (Figure 1g). The inner diameter of the microring is ≈30 μm, and the outer diameter is ≈82 μm.

To demonstrate the feasibility of substrate–cell interactions, two representative cells were guided by micropillar scaffolds: neurons differentiated from NSCs and hippocampal neurons. Neurons differentiated from NE-4C NSCs have a larger soma size and wider neurite diameter than primary cultures of hippocampal neurons. Moreover, NSCs can have serial passages; therefore, the stability and repeatability of the experiment are high.

Micropillar scaffolds with different spacings are designed to guide axonal and dendritic growth of neurons differentiated from NE-4C NSCs. We found that the neurite orientation distribution on micropillar scaffolds with a distal distance of 3 μm was arbitrary and did not observe promoting effects of NSC neurite growth compared with cells growing on a glass substrate. When the distal distance increases to 6 or 9 μm, most of the neurites are parallel to the proximal axis when imaged using scanning electron microscopy (SEM) (Figure 1h,j). Its neurite length is longer than those on micropillars with a distal distance of 3 μm. When the distal distance increases to 12 μm, SEM shows that part of the NSC somas fall directly on the top of the micropillars and most neurites grow along the proximal axis of the micropillars (Figure 1i,k). Furthermore, interactions were observed between the nerve cells and the micropillars, and the micropillars were tilted under the action of the force (Figure S1, Supporting Information).

2.2. Neuron Growth Morphology Regulated by Micropillar Scaffolds with Different Spacings
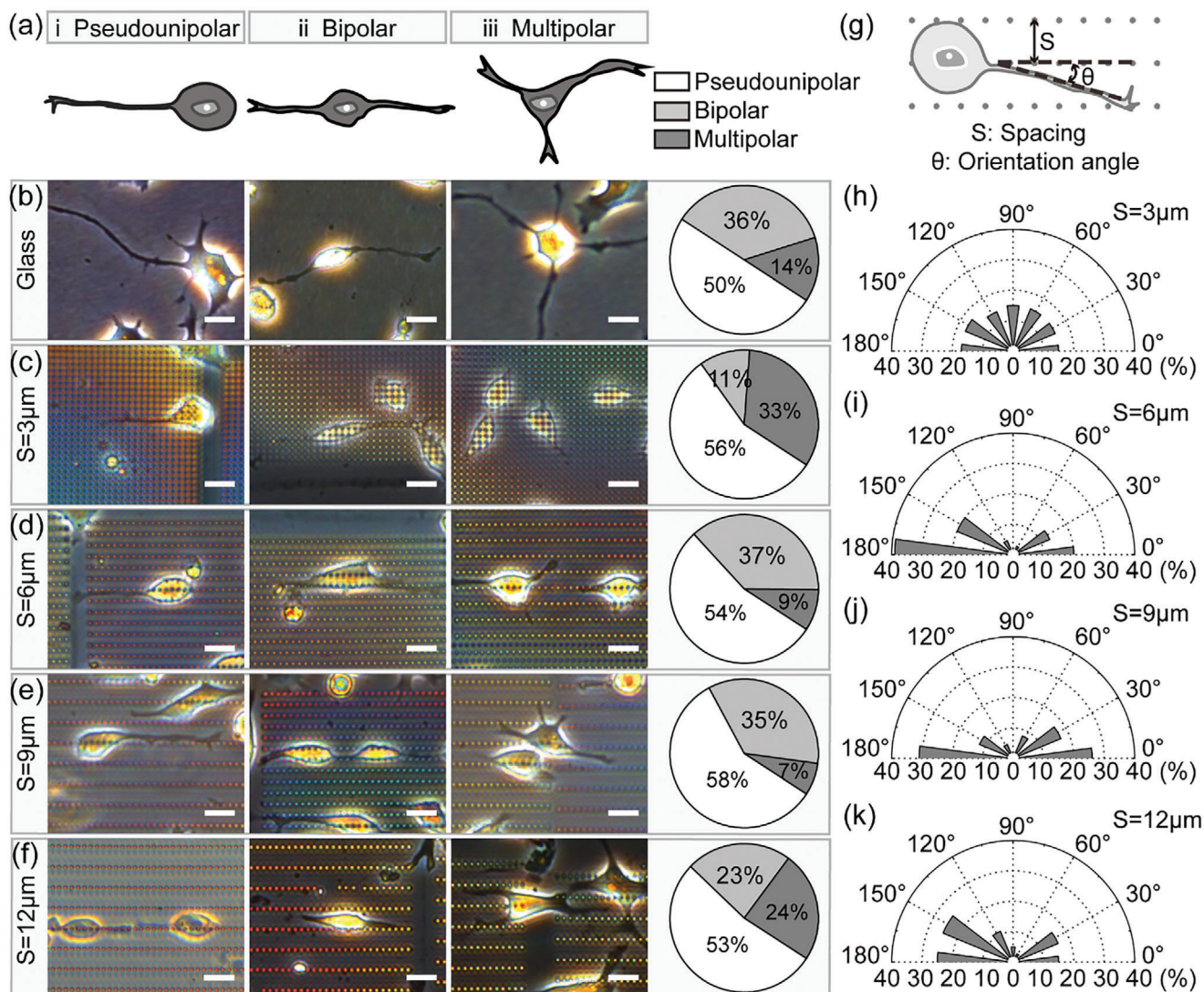
For NE-4C mouse NSC-differentiated neurons, micropillar scaffolds of various spacings affect axon and dendrite branching, orientation and length. In neuronal development, a key mechanism
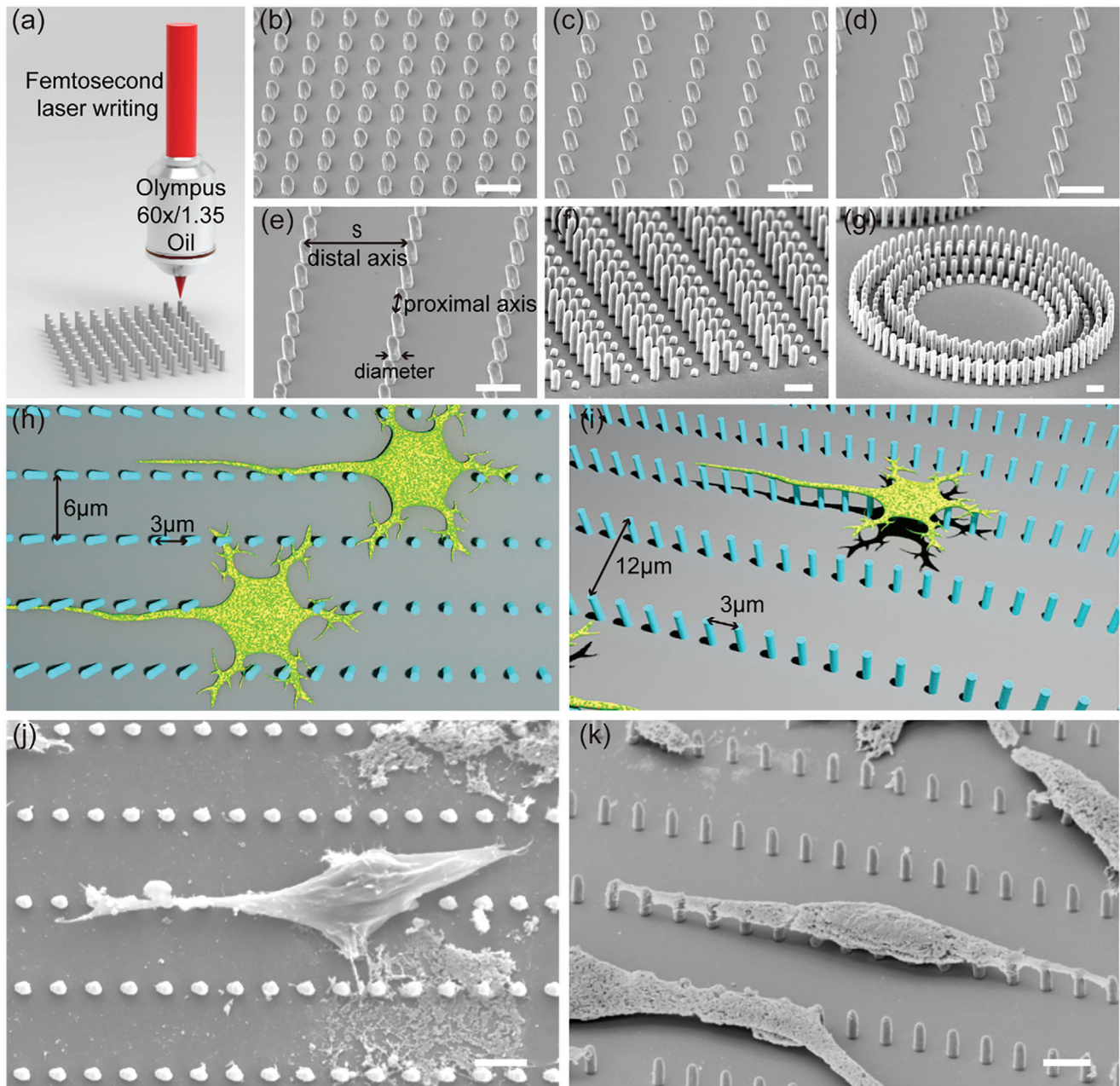
Figure 1. Micropillar scaffolds guide the directional growth of neurons. a) Schematic diagram of fabrication. b–e) Scanning electron microscopy (SEM) of anisotropic micropillar scaffolds and scaffolds with proximal distances of 3 µm and distal distances of 3, 6, 9, and 12 µm. Micropillars with a height of 6 µm and diameter of 1 µm. e) Distal distance (*S*) of the micropillar refers to the distance between two distal axes. f) SEM image of 3D micropillar scaffolds with different heights. Micropillars with a spacing of 3 µm and heights of 2, 4, and 6 µm. g) Micropillars with heights of 3, 6, and 9 µm. The micropillars are patterned to form 3D microrings with an inner diameter of 30 µm and an outer diameter of 82 µm. h,i) Schematic diagram of cell growth on anisotropic micropillar scaffolds. The proximal distance of the scaffolds was 3 µm, and the distal distances of the scaffolds were 6 and 12 µm. j,k) SEM images of NE-4C mouse neural stem cells (NSCs) cultured for 4 days in vitro (DIV) on anisotropic micropillar scaffolds. j) Micropillar scaffolds with a distal distance of 6 µm guide neurite growth. k) Micropillar scaffolds with a distal distance of 12 µm guide neurite growth. Scale = 4 µm.

is the ability of the motor growth cones at the tip of the growing process to measure environmental cues and use them to grow accordingly. Using the micropillar scaffold as an environmental signal, we think that the growth cone can couple the intracellular movement signal to the fixed extracellular scaffold via cell surface adhesion receptors and then move forward in a directional direction. By observing the movement direction of the growth cone, the influence of micropillar scaffolds with different spacings on the branching, orientation and length of neuron neurites differentiated by NSCs was studied. **Figure 2**a shows a schematic

**ADVANCED
SCIENCE NEWS**

www.advancedsciencenews.com

**ADVANCED
HEALTHCARE
MATERIALS**

www.advhealthmat.de

Figure 2. Neuron growth morphology is regulated by micropillar scaffolds with different spacings. a) Schematic diagrams of NSCs with pseudounipolar, bipolar, and multipolar morphologies. b–f) Left three panels: phase contrast graphs show the NSC growth morphology at 3 DIV; right panel: pie charts show the percentage of neurite branches on glass substrates and micropillar scaffolds with spacings of 3, 6, 9, and 12 μm (n = 100, 134, 100, 87, and 97 cells correspond to glass substrates and micropillar spacings of 3, 6, 9, and 12 μm, respectively, with nine separate cultures). g) Schematic diagram of micropillar spacing (S) and growth orientation (θ). The orientation of neurites is represented by the orientation angle distribution. The orientation angle θ of each neurite is measured as the angle between the neurite vector and the proximal axis of the image plane. h–k) Wind rose diagrams illustrate the relative frequency distribution in the orientation of neurites (n = 134, 100, 87, and 97 cells correspond to spacings 3, 6, 9, and 12 μm, respectively, with nine separate cultures). The number of cells near a specific angle value is expressed as a percentage of cells. The Origin software package was used for the statistical analysis. Scale = 20 μm.

of NSC-differentiated neurons with pseudounipolar, bipolar, and multipolar morphologies. Phase contrast images and pie charts show the relative frequency distribution of the number of neurite branches (Figure 2b–f). The growth orientation of neurites at distal distances of 3, 6, 9, and 12 μm was quantitatively evaluated. A schematic diagram of Figure 2g shows the neurite length and growth orientation. The relative frequency distribution of the orientation of axons and dendrites on micropillar scaffolds with different spacings is shown by wind rose diagrams. The histogram illustrates the length distribution of neurites on glass substrates and micropillar scaffolds with different spacings for 1 day and

2 days in vitro (DIV). Here, DIV is short for day in vitro, it referred to the number of in vitro culture days (see Figure S2, Supporting Information).

When the distal distance of the micropillar scaffolds is 3 μm, the proportions of pseudounipolar, bipolar and multipolar neurite branches are 56%, 11%, and 33%, respectively. Compared with neurite branches on other micropillars, neurites have the fewest bipolar branches and more multipolar branches. Neurite orientation is almost evenly distributed from 0° to 180°, and the percentages of neurite orientation angles near 0° and 180° are only 15% and 17%, respectively (Figure 2h). The neurite

length is even shorter than that of neurites on glass substrates. When the distal distance increases to 6 µm, the proportions of pseudounipolar, bipolar and multipolar branches on micropillar scaffolds are 54%, 37%, and 9%, respectively. Compared with neurites on micropillars with a spacing of 3 µm, the number of multipolar branches is reduced and the number of bipolar branches is increased. The orientation angles of neurites at 0° and 180° accounted for 59%; therefore, the neurite growth direction gradually tended toward consistency (Figure 2i). The neurite length is slightly longer than that of neurites on the other substrates. A combination of increasing neurite length and reducing neurite branching supports a strong guidance effect and directional growth of neurons on micropillars with a spacing of 6 µm. When the distal distance increases to 9 µm, the proportions of pseudounipolar, bipolar and multipolar branches on micropillar scaffolds are 58%, 35%, and 7%, respectively. Compared with other substrates, the proportion of multipolar neurites is the smallest. In the distribution of neurite orientation, 0° and 180° accounted for 57%. Therefore, the direction of neurite growth still tends to be consistent (Figure 2j). The neurite length is longer than that of neurites on glass substrates. When the distal distance is 12 µm, the proportions of pseudounipolar, bipolar and multipolar branches are 53%, 23%, and 24%, respectively. The number of multipolar branches increased slightly, but there were still fewer branches than neurites on micropillar scaffolds with a spacing of 3 µm. Although neurite has no obvious orientation angle, the orientation is more consistent than the orientation of neurites on micropillar scaffolds with a spacing of 3 µm (Figure 2k). The neurite length is slightly longer than that of neurites on glass substrates.

Neuronal growth is affected by the micropillar scaffold, and the interactions between micropillars and cells control the branching, orientation and length of neurons. The interactions between neurons and micropillars with different spacings indicate that the strength of the interaction is related to the spacings of the micropillars. In short, the anisotropic micropillar scaffolds reduce neurite branching and slightly elongate neurite length. Importantly, most NSC neurites have a consistent orientation angle, which is crucial for the formation of neuronal networks.

2.3. Long-Term Directional Growth of Hippocampal Neurons Guided by Micropillar Scaffolds

Long-term primary culture of isolated neurons has proven to be a valuable tool for studying neuron development and function.[23,24] In culture, another representative hippocampal neuron cell is selected. Hippocampal neurons are typical cells used to study the effects of biochemical and physical signals on axon and dendrite growth. Hippocampal neurons were cultured on poly-L-lysine-and laminin-coated micropillar scaffolds with the same height and various spacings and labeled by immunofluorescence markers for axons and dendrites (tau) and somas and dendrites (Map2) at 13 days in vitro (DIV). Map2 was found in somas and dendrites, but by contrast tau was just enriched in axons. When the distal distance was 6 µm, the axons and dendrites of hippocampal neurons were mostly aligned with the proximal axis and some axons and dendrites grew along the top of the micropillars (**Figure 3**a; Figure S3a, Supporting Infor-

mation). The distance of 6 µm between the micropillars is also the size of the hippocampal neuron growth cone;[25] therefore, we inferred that axons preferred to interact with micropillars available within a growth cone-sized range (Video S1, Supporting Information). As shown in Figure 3b, hippocampal neurons grew on a flat glass substrate served as a control group and axons and dendrites of neurons grew irregularly on a glass substrate.

When the distance between the distal axis of the micropillar scaffold is 12 µm, some axons and dendrites can also grow along the top of the micropillars (see Figure S3c, Supporting Information) and the orientation of most neuronal neurites is also along the proximal axis (Figure 3c). In micropillar scaffolds, the distal distance is much larger than the proximal distance; therefore, neurites may follow the existing contact points to find the nearest contact point. Therefore, the initial position of the neuron and the relative position between the neuron and micropillar scaffold result in neurite patterning, especially neurite alignment along the proximal axis. Hippocampal neurons grew in a disordered manner on a glass substrate were used as the control group (Figure 3d).

In terms of neurons, it is necessary to develop a culture scaffold that can culture primary neurons for a long time to meet potential applications.[26] We further clarified the influence of culture days on the orientation angle of neuron axons and dendrites on micropillar scaffolds. Neurons were cultured for 3, 7, 10, and 13 DIV, and the orientation angles of axons and dendrites on micropillar scaffolds with spacings of 6 and 12 µm were calculated. At 3 DIV, the growth orientation of hippocampal neurons reached 45% along the proximal axis (0° and 180°) (Figure 3e). At 7 DIV, the growth orientation of hippocampal neurons increased to 53% in the proximal axis direction (Figure 3f). After in vitro culture for 10 days, the ratio parallel to the proximal axis was as high as 56% (Figure 3g). Even after 13 DIV, neurons grew well and had almost no apoptosis (Figure 3h). Therefore, discontinuously anisotropic micropillar scaffolds were treated with reagents, and the micropillar scaffolds were biocompatible for neuron culture and supported axon and dendrite growth, which can be observed as directional growth of axons and dendrites for a long time.

The results indicate that neurons differentiated from NSCs and hippocampal neurons have the same orientation on micropillar scaffolds with distal distances of 6 and 12 µm, respectively. Micropillar scaffolds can guide directional growth of neuron axons and dendrites for a long time.

2.4. Directional Growth of Neurons to Form Neuronal Networks Guided by Patterned Micropillar Scaffolds with Different Heights

While a 2D micropillar scaffold can guide the patterned growth of neurons, as discussed above, a 3D cell scaffold is closer to an in vivo environment. The influence of 3D micropillar scaffolds with different heights on the hippocampal neurite orientation angle was therefore studied. Here, the heights of 3D micropillar scaffolds were 3, 6, and 9 µm and 2, 4, and 6 µm, respectively. Hippocampal neurons grew on micropillars with the same spacing and various heights at 7 DIV and were stained for immunofluorescence. When the heights of the micropillars were 3, 6, and 9 µm, hippocampal neurites grew directionally along micropillars with the same height (**Figure 4**a). Axons and dendrites grew
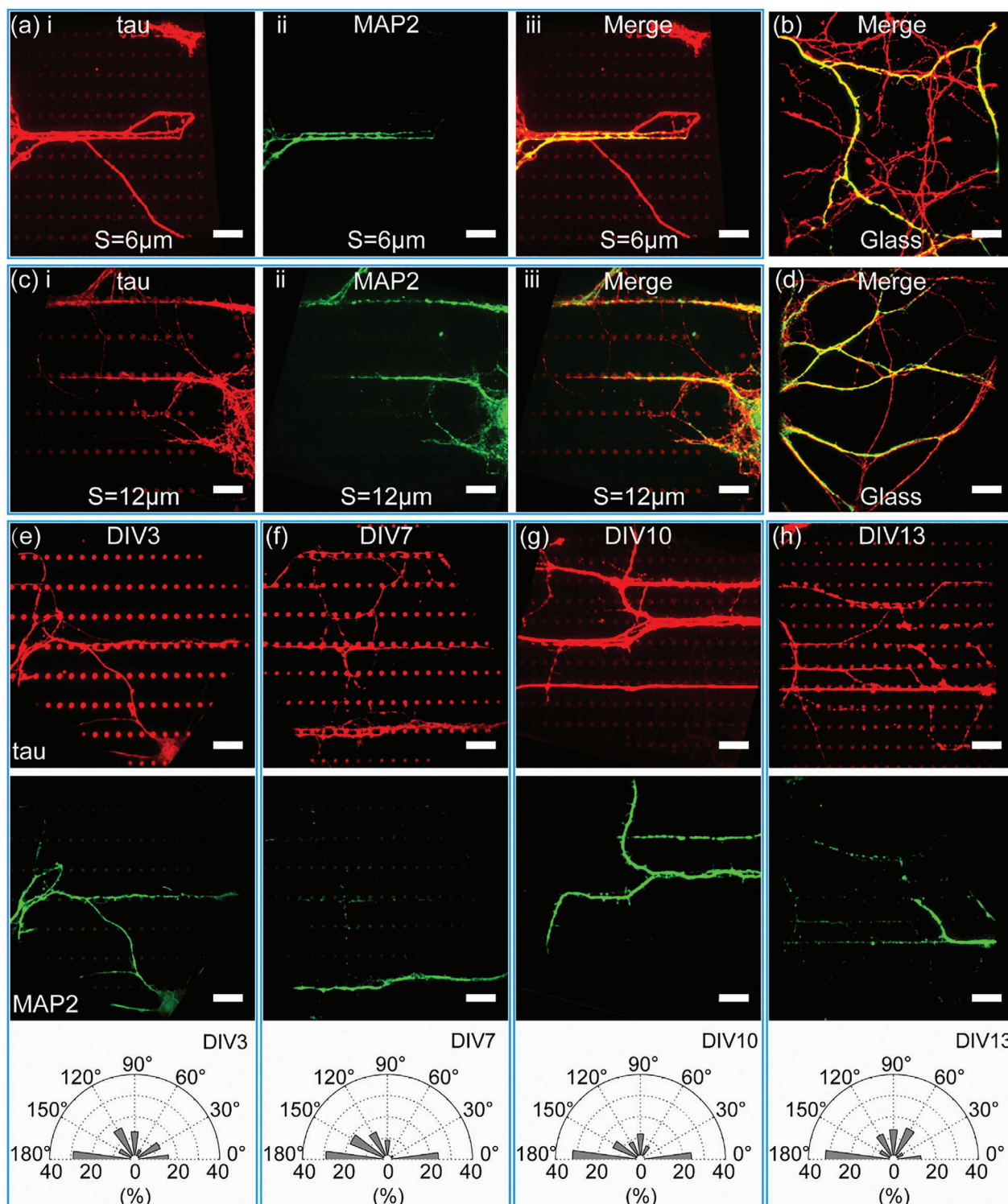
Figure 3. Long-term directed growth of hippocampal fetal rat neurons is guided by micropillar scaffolds with different spacings. a) Orientation of neurite growth on poly-L-lysine- and laminin-coated micropillars. Micropillars with a distal distance of 6 µm. From left to right: antibody labeled tau (red), antibody labeled Map2 (green), and merged panels combining two images, Tau and Map2. b) Glass substrate as a control group. c) Micropillars with a distal distance of 12 µm. From left to right: antibody labeled tau (red), antibody labeled Map2 (green), and merged panels combining two images, Tau and Map2. d) Glass substrate as a control group. e–h) Representative fluorescence microscopy images showing micropillars with a distal distance of 6 µm guide neuron growth at 3, 7, 10, and 13 DIV. From top to bottom: antibody labeled tau (red) and antibody labeled Map2 (green). The wind rose diagrams illustrate the relative frequency distribution of the orientation of neurites ($n = 124, 136, 77$, and 90 neurites correspond to 3, 7, 10, and 13 DIV, respectively, with nine separate cultures). The Origin software package was used for the statistical analysis. Scale = 10 µm.
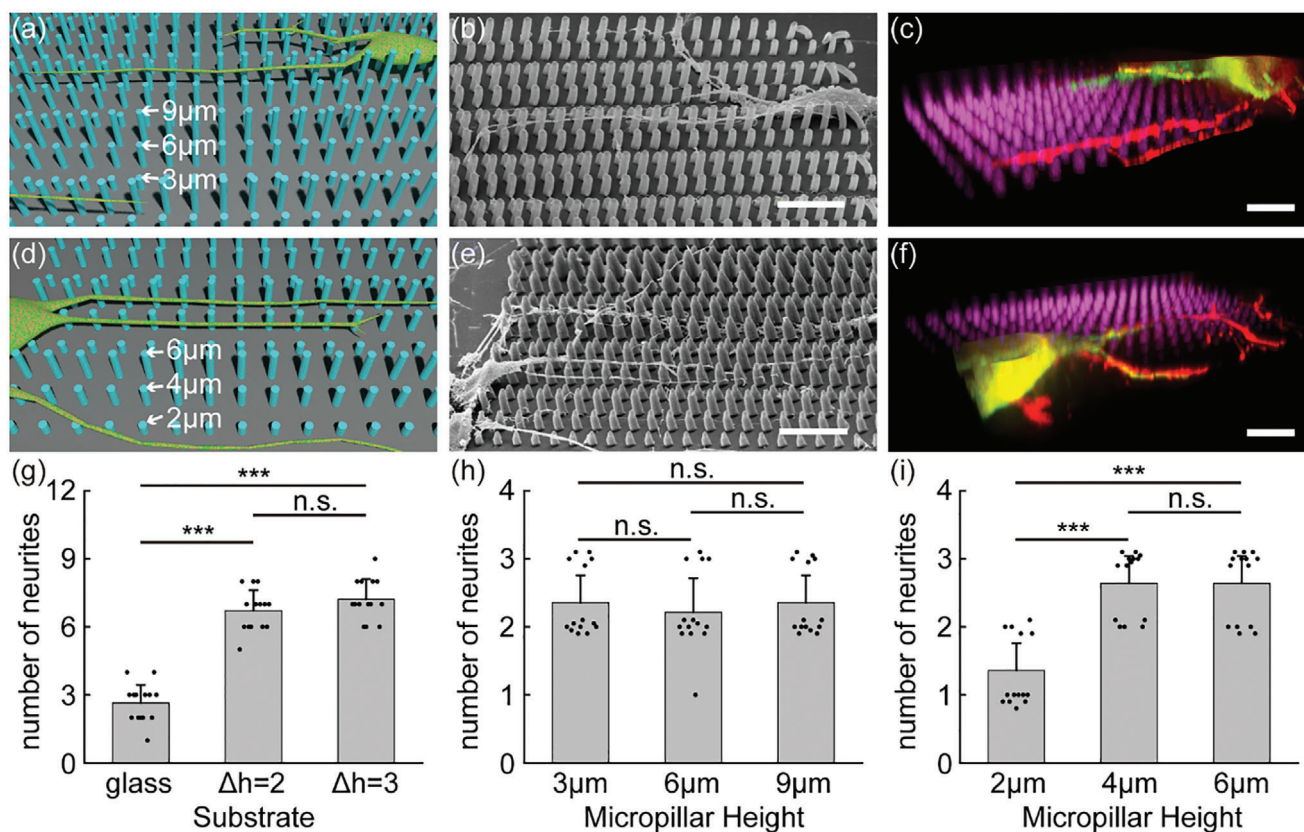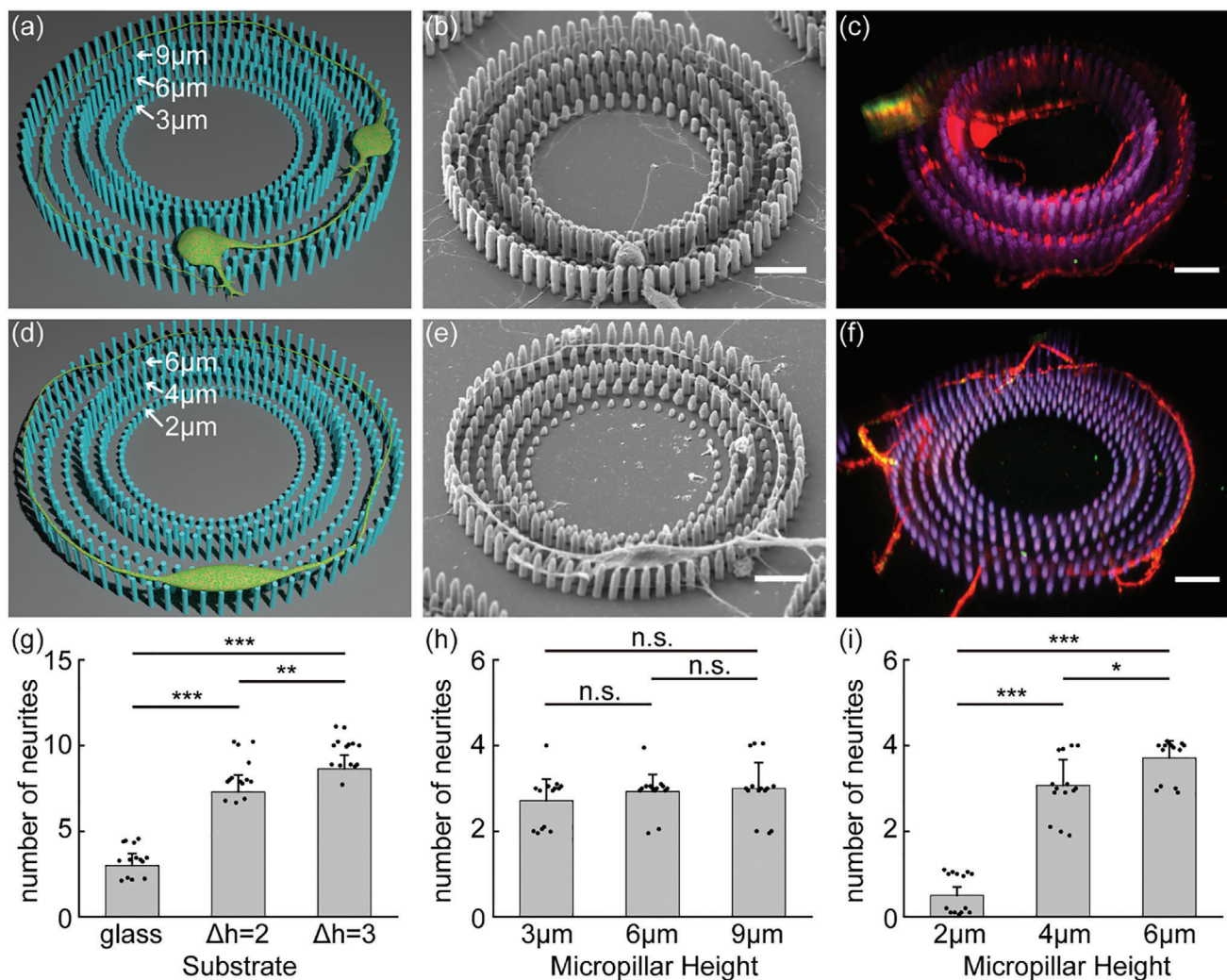
Figure 4. Directional growth of neurons is guided by micropillar scaffolds with different heights. a–c) Micropillars with a proximal distance of 3 µm, distal distance of 3 µm, diameter of 1 µm and heights of 3, 6, and 9 µm. a) Schematic diagram of neuron growth on micropillar scaffolds. b) SEM image shows that hippocampal neurites were cultured at 7 DIV on 3D micropillar scaffolds. c) Immunofluorescence staining of hippocampal neurons at 7 DIV. Neurite is stained with tau (red), and Map2 (green), and micropillars are shown in purple. d–f) Neuron growth on 3D micropillar scaffolds with heights of 2, 4, and 6 µm. d) Schematic diagram of neuron growth on micropillar scaffolds. e) SEM image shows that hippocampal neurites were cultured at 7 DIV on 3D micropillar scaffolds. f) Immunofluorescence staining of hippocampal neurons at 7 DIV. g) Number of neurites grown on glass substrates and micropillar scaffolds with height differences of 2 and 3 µm. h) Number of neurites growing on micropillar scaffolds with heights of 3, 6, and 9 µm. i) Number of neurites growing on micropillar scaffolds with heights of 2, 4, and 6 µm. g–i) Number of neurites ± SD in the indicated area, $n = 14$ samples, with five separate cultures. Actual measured values are expressed by scattered points, without preprocessing of data. The Origin software package was used for the statistical analysis, followed by one-way ANOVA; *$p < 0.05$, **$p < 0.01$, ***$p < 0.001$, and n.s., no significance. Scale = 10 µm.

along the sidewall of micropillars of the same height, although that hippocampal neurons fell on the sidewall of the micropillar (Figure 4b). The 3D immunofluorescence image (Figure 4c) confirms that hippocampal neurons are guided by micropillar scaffolds to grow directionally. The growth pattern of axons and dendrites may be closely related to the initial position of the soma and the relative position between the neurons and micropillars. A possible reason is the large height difference between micropillars, which will cause the neurite to be aligned at the same height. Hippocampal neurons were cultured on a glass substrate, which served as the control group, and the neuronal axons and dendrites grew in a disordered manner on a glass substrate (see Figure S4a,b, Supporting Information). The number of neurites on a glass substrate was significantly lower than that on the micropillar scaffolds (Figure 4g). The number of neurites growing on 3D micropillar scaffolds with heights of 3, 6, and 9 µm was counted (Figure 4h). Significant differences were not observed in the number of neurites growing on 3D micropillar scaffolds with different heights, which indicated that the neurites were almost uniformly distributed and grew directionally on 3D micropillar scaffolds with a height difference of 3 µm.

When the heights of micropillars were 2, 4, and 6 µm, the growth directions of axons and dendrites were mainly parallel to micropillar scaffolds of the same height (Video S2, Supporting Information). Neurons tended to grow along micropillars with heights of 4 and 6 µm, and only a few axons and dendrites grew along micropillars with a height of 2 µm (Figure 4d–f). Neurite growth on micropillar scaffolds with a height of 2 µm was significantly different from that on micropillar scaffolds with heights of 4 and 6 µm (Figure 4i). Neurites grew selectively and directionally on the micropillar scaffold with a height difference of 2 µm and a minimum height of 2 µm. The selection of neurite growth was mainly related to the initial position of somas and the height of micropillar scaffolds. Hippocampal neuron growth on a glass substrate served as the control group, and axons and dendrites of neurons grew irregularly on a glass substrate (see Figure S4c,d, Supporting Information). Moreover, even if the heights of micropillars were 6, 9, and 12 µm, axons and dendrites tended to
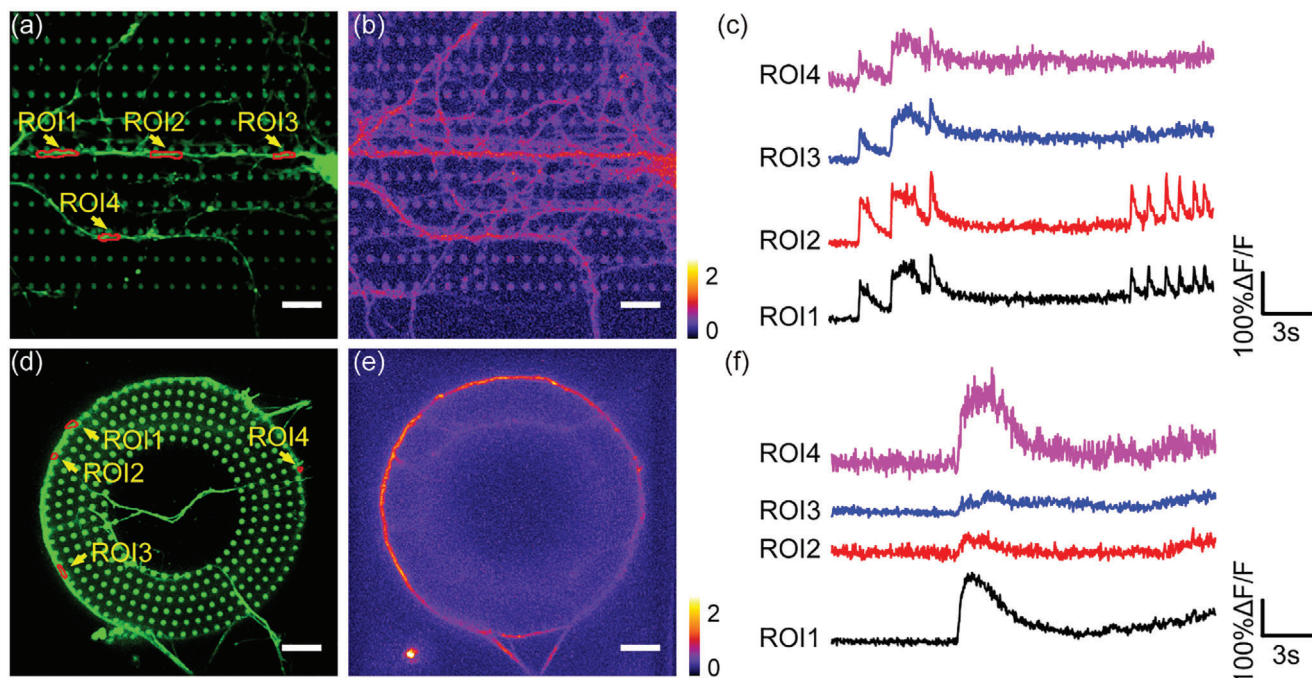
Figure 5. Directional growth of neurons to form neuronal networks is guided by patterned 3D microring scaffolds with different heights. a–c) Micropillars with a proximal distance of 3 µm, distal distance of 3 µm, and diameter of 1 µm. The micropillars are patterned to form microrings, the toroid inner diameter is 30 µm, the outer diameter is 82 µm and the heights are 3, 6, and 9 µm. a) Schematic diagram of neuron growth on microring scaffolds. b) SEM image shows that neurites were cultured at 7 DIV on microring scaffolds. c) Immunofluorescence staining of hippocampal neurons at 7 DIV. Neurite stained with tau (red) and Map2 (green), and micropillars are shown in purple. d–f) Neuron growth on 3D microring scaffolds with heights of 2, 4, and 6 µm. d) Schematic diagram of neuron growth on microring scaffolds. e) SEM image shows that neurites were cultured at 7 DIV on microring scaffolds. f) Immunofluorescence staining of hippocampal neurons at 7 DIV. g) Number of neurites grown on glass substrates and microring scaffolds with heights differences of 2 and 3 µm. h) Number of neurites growing on microring scaffolds with heights of 3, 6, and 9 µm. i) Number of neurites growing on microring scaffolds with heights of 2, 4, and 6 µm. g–i) Number of neurites ± SD in the indicated area, $n = 14$ samples, with five separate cultures. Actual measured values are expressed by scattered points, without preprocessing of data. The Origin software package was used for the statistical analysis, followed by one-way ANOVA; *$p < 0.05$, **$p < 0.01$, ***$p < 0.001$, and n.s., no significance. Scale = 10 µm.

grow along micropillars with the same height. In particular, micropillar scaffolds with different heights can guide the growth of neurons to form autaptic neurons (see Figure S5a, Supporting Information).

To encourage neurons that form circular neuronal circuits in a 3D environment, a novel 3D microring scaffold composed of micropillars of different heights is fabricated to investigate the effect of micropillar height on the selective growth of hippocampal neurons. We designed linear micropillar scaffolds of various heights with a constant spacing of 3 µm between the micropillars. The heights of the microrings composed of micropillars are 3, 6, and 9 µm (**Figure 5**a). Interestingly, the experimental results

for 3D microrings are consistent with the linear micropillar scaffolds. Neurites also tend to grow directionally along micropillars at the same height, and the growth direction of neurites is related to the initial position of the soma. For example, when neurons fall on micropillars with a height of 6 µm, they prefer to grow along micropillars with a height of 6 µm rather than along micropillars with heights of 3 and 9 µm (Figure 5b). The 3D immunofluorescence image (Figure 5c) confirms that hippocampal neurons are guided by microring scaffolds to grow directionally. Hippocampal neurons cultured on a glass substrate served as a control group, and axons and dendrites of neurons grew irregularly on a glass substrate (see Figure S6a,b, Supporting

**ADVANCED
SCIENCE NEWS**

www.advancedsciencenews.com

**ADVANCED
HEALTHCARE
MATERIALS**

www.advhealthmat.de

Figure 6. Monitoring neuronal activity in networks by Ca^{2+} imaging. a–c) Fluo8 labeled hippocampal neurons (13 DIV) on micropillars with a proximal distance of 3 µm and distal distance of 6 µm. (a,b) Spatial distribution of the Ca^{2+} activity of hippocampal neurons at different positions. (a) Four neurite sites are marked with red closed curves in the confocal image. (b) Pseudocolor MIP (maximum intensity projection) image of the fluorescence change ($\Delta F/F_{median}$) shows the fluorescence intensity change of hippocampal neurons during 1 min, and the bright color region represents the neuronal action potential that occurred in this period. c) Ca^{2+} imaging $\Delta F/F$ trace of 4 ROIs. d–f) Fluo8-labeled hippocampal neurons (13 DIV) on 3D microrings with a distance of 3 µm on the proximal axis, a distance of 3 µm on the distal axis, and heights of 2, 4, and 6 µm. (d,e) Spatial distribution of the Ca^{2+} activity of neurites at different positions. (d) Four neurite sites are marked with red closed curves in the confocal image. (e) Pseudocolor MIP (maximum intensity projection) image of the fluorescence change ($\Delta F/F_{median}$) shows the fluorescence intensity change of hippocampal neurons. (f) Ca^{2+} imaging $\Delta F/F$ trace of 4 ROIs. The Origin software package was used for the statistical analysis. Scale = 10 µm.

Information). Neurite growth on glass substrates was also significantly less than that on micropillar scaffolds (Figure 5g). The number of neurites growing on 3D microring scaffolds with heights of 3, 6, and 9 µm was not significantly different (Figure 5h). Neurites grow directionally on micropillar scaffolds with a height difference of 3 µm.

Similarly, 3D microring scaffolds with heights of 2, 4, and 6 µm were designed to guide the growth of neurites (Figure 5d; Video S3, Supporting Information). Figure 5e,f shows that most axons and dendrites can be guided by microrings to form autaptic neurons. Experimental results show that most neurites also grow along the direction of 3D microrings composed of micropillars with heights of 4 and 6 µm and directly pass through microrings with a height of 2 µm. Neurite growth on the microring scaffolds with a height of 2 µm was significantly less than that on the microring scaffolds with heights of 4 and 6 µm (Figure 5i). Therefore, we speculate that neurites are not sensitive to micropillar scaffolds with a height of 2 µm. More importantly, the ratio of linear micropillar scaffolds forming autaptic neurons was less than 1%, and the ratio of microring scaffolds forming autaptic neurons was more than ≈50% (Figure S7, Supporting Information). Therefore, compared to linear micropillar scaffolds, autaptic neurons are more easily formed by microring-guided neurites. Hippocampal neurons cultured on a glass substrate served as a control group, and axons and dendrites of neurons grew irregularly on a substrate (Figure S6c,d, Supporting Information).

In summary, when the height difference between the micropillars was 3 µm, neurites mainly grew along patterned micropillar scaffolds with the same height. When the height difference between micropillars was 2 µm and the minimum height of the micropillar was 2 µm, neurites tended to grow along patterned micropillar scaffolds with heights of 4 and 6 µm, and passed through micropillars with a height of 2 µm. Therefore, patterned 3D micropillar scaffolds can guide the directional growth of neurons to form autaptic neurons. In particular, patterned 3D microring scaffolds more easily form autaptic neurons than linear micropillar scaffolds, thus providing an experimental method that allows the quantitative assessment of input and output properties of individual neurons, both in morphological and functional experiments.

2.5. Monitoring Synaptic Signal Transmission in 3D Directional Neuronal Networks by Spontaneous Ca^{2+} Activity

Functional Ca^{2+} imaging is widely used to monitor nerve cell activity in vitro and in vivo.[27] Synaptic signal transmission is monitored on micropillar scaffolds with a distal distance of 6 µm and proximal distance of 3 µm (Video S4, Supporting Information). In the confocal image of the neuronal network, spontaneous changes in Ca^{2+} at 4 neurite sites were measured (**Figure 6**a). The pseudocolor (maximum intensity projection (MIP) image of the fluorescence change ($\Delta F/F_{median}$) indicates the change in calcium

**ADVANCED
SCIENCE NEWS**

www.advancedsciencenews.com

**ADVANCED
HEALTHCARE
MATERIALS**

www.advhealthmat.de

concentration in hippocampal neurons (Figure 6b). By analyzing the spontaneous Ca^{2+} activity of hippocampal neuronal axons and dendrites, the Ca^{2+} fluorescence intensity at sites 1 to 4 on the micropillars was almost the same in the first 2 s in Figure 6c, which shows strong connectivity between the neurons showing synchronized firing. This finding indicates that a burst of activity occurs between neuronal networks guided by micropillars caused by synaptic transmission. However, in the last 1 s of recording, the spontaneous Ca^{2+} fluorescence intensity peaks of hippocampal neurons only occurred at sites 1 and 2 (Figure 6c). The different firing patterns of neurons may reflect different synaptic connections between discordant neurons.

Synaptic signal transmission is monitored on 3D microring scaffolds composed of micropillars with a spacing of 3 μm and heights of 2, 4, and 6 μm (Video S5, Supporting Information). The spontaneous changes in Ca^{2+} at four neurite sites in the formed network were measured by confocal imaging (Figure 6d). The pseudocolor MIP image of the fluorescence change ($\Delta F/F_{median}$) indicates the activity of hippocampal neurons (Figure 6e). We found that the change in Ca^{2+} fluorescence intensity at sites 1 to 4 on the micropillars was similar, thus indicating strong connections between microring-guided neurons (Figure 6f). In addition, experiments also showed that the change of Ca^{2+} fluorescence intensity at sites 1 to 4 on the microrings was similar, the action potentials were emitted synchronously; therefore, neuron cells formed functional neuronal networks (Figure S8, Supporting Information).

Based on the analysis of spontaneous Ca^{2+} activity of neurons, a burst of activity occurs between neuronal networks under the guidance of micropillars, which proves that the burst of activity between neurons is caused by synaptic transmission. In short, micropillars of various spacings and heights can guide neurite directional growth, thus increasing the likelihood of synaptic connectivity between neurons. The above results demonstrate that our method is useful for a neuronal network analysis platform.

3. Conclusions

In summary, using one-step fs-DLW, we successfully fabricated discontinuous, anisotropic micropillar scaffolds with different spacings and heights. These scaffolds have a guiding effect on NE-4C mouse NSC differentiated neurons and hippocampal neurons for a long time. Micropillar scaffolds of various spacings reduce neurite branching, and most of the axons and dendrites have an orientation angle parallel to the proximal axis. Furthermore, 3D micropillar scaffolds with different heights are used to guide the growth patterns of axons and dendrites to form neuronal circuits. More importantly, neurites guided by a microring scaffold more easily form autaptic neurons than linear micropillar scaffolds. Calcium imaging shows that there are synchronized firing patterns and strong connectivity between neurons guided by 3D micropillar scaffolds, which is of great significance to the study of mechanical transduction pathways and neuronal networks in neuronal synaptic connections. This method can guide the directional growth of neurons to form neuronal networks, which has wide applications, including synaptic signaling, nerve repair, and neural tissue engineering. It is especially suitable for studying the behavior of cells in a 3D environment, such as the

orientation and branching of neurons, both of which are important aspects to be considered in future research.

4. Experimental Section

Substrate Preparation: A regenerative amplified Ti:sapphire femtosecond laser system (Legend Elite-1K-HE, Coherent, USA) with a 75 fs pulse width, 80 MHz repetition rate and 800 nm central wavelength was employed to fabricate micropillar scaffolds using SZ2080 photoresist.[28] First, the photoresist was dropped on a coverslip, and then subjected to a baking treatment at 100 °C for 1 h to remove the solvent. Then, micropillars on glass substrates were manufactured by focusing the femtosecond laser beam through a 60× oil-immersion objective lens (Olympus, numerical aperture (NA) 1.35) for two-photon polymerization into the photoresist. Fs-DLW technology can flexibly fabricate 3D micropillar scaffolds of various spacings and heights. A single micropillar was polymerized on a glass surface with a laser power of 9 mW.

After fabrication, the unexposed region of the photoresist was dissolved by washing the glass coverslips with 1-propanol solution development, and then the cover glass was washed with Dulbecco's phosphate-buffered saline (DPBS). For the cell experiments, the patterned samples were sterilized by immersion in 75% ethanol followed by UV light irradiation for 30 min. Since poly-L-lysine can facilitate cell adhesion to solid surfaces,[29] these micropillars were coated with poly-L-lysine (20 μg mL^{-1}, Sigma-Aldrich) overnight at 4 °C, followed by washing twice with DPBS. Finally, because laminin was the main substrate for axon growth in vivo and in vitro,[30] the micropillars were coated with a solution of laminin (20 μg mL^{-1}, Sigma-Aldrich) at 4 °C for 12 h and washed with DPBS before cell seeding.[31]

Cell Cultures: The NE-4C mouse NSC line was derived from the vesicles of 9-day p53-function gene knockout mouse embryos (NE-4C mouse NSCs were kindly provided by Stem Cell Bank, Chinese Academy of Sciences). To increase the proportion of neurons differentiated from NSCs, the effects of different concentrations of fetal bovine serum and different types of coated proteins on cell proliferation and differentiation were tested. Finally, NE-4C NSC lines were maintained on poly-L-lysine- and laminin-coated dishes in minimum essential medium (MEM; Invitrogen) supplemented with 1% fetal bovine serum (FBS; Gibco), 1% Glutamax (Invitrogen), 1% nonessential amino acids, 100× (Invitrogen), 20 ng mL^{-1} NGF (nerve growth factor),[32] 100 U mL^{-1} penicillin, and 100 μg mL^{-1} streptomycin.[33] Differentiation medium was replaced every 2 days, and NE-4C mouse NSCs were differentiated into neurons and astrocytes in differentiation medium.[34]

Preparation of low density dissociated embryonic rat hippocampal neurons followed a previous protocol.[35] In brief, hippocampi of embryonic day-18 embryos (without distinguishing sex differences) from pregnant Sprague-Dawley rats (CD (SD) IGS, Beijing Vital River Laboratory Animal Technology Co. Ltd., Beijing, China) were dissected and treated with 0.25% trypsin (Sigma-Aldrich) for 15 min at 37 °C. DMEM (Biowhittaker) supplemented with 10% F12 (Biowhittaker), 10% heat-inactivated fetal bovine serum (Thermo Fisher) and 1× B27 (Thermo Fisher) was used as the culture medium. The dissociated cells were seeded on poly-L-lysine- and laminin-coated micropillar substrates on Φ18 mm coverslips (Assistent) in 35 mm petri dishes at a density of 30 000–50 000 cells mL^{-1} and maintained in incubators at 37 °C in 5% CO_2. Culture medium (1.5 mL) was added to each dish. Twenty-four hours after seeding, half of the medium was replaced with serum-free NeuroBasal (NB) medium (Thermo Fisher) supplemented with 1× Glutamax (Thermo Fisher) and 1× B27 (Thermo Fisher), and then half of the medium was replaced with fresh serum-free NB culture medium every 3 days. Cytosine arabinoside (Sigma-Aldrich) was added to the culture for 3 days in vitro (final concentration, 2×10^{-6} M) to prevent overgrowth of glial cells. All experiments were performed on neurons at 2–13 DIV and repeated on 2 or more separate cultures unless otherwise specified. All animal experiments were approved by the Animal Experiments Committee at the University of Science and Technology of China (USTCACUC152101034).

**ADVANCED
SCIENCE NEWS**

www.advancedsciencenews.com

**ADVANCED
HEALTHCARE
MATERIALS**

www.advhealthmat.de

Biological Testing: For immunofluorescence staining, neurons were fixed for 20 min with cold 4% paraformaldehyde in PBS (0.01 mol L^{-1} phosphate buffer solution, pH = 7.4) in an imaging chamber, washed with PBS and permeabilized with Triton X-100 (0.2% Triton X-100 in PBS). Fixed and permeabilized neurons were blocked in 3% BSA in PBS for 1 h and primary antibodies were applied in 3% BSA in PBS overnight at 4 °C. Samples were washed with PBS and then incubated with secondary antibodies in 3% BSA for 45 min at room temperature. The following primary antibodies were used: guinea pig anti-tau (1:1000; SYSY 314004) and mouse anti-map2 (1:500; Sigma-Aldrich M4403). Labeled secondary antibodies were raised in donkey against the appropriate species and conjugated to Alexa 488 (1:400; Jackson lab 706-545-148) or Alexa 640 dyes (1:800; Jackson lab 715-605-151).[36] Stained cells were visualized under a fluorescence microscope (Olympus IX-81-ZDC, Japan) equipped with a 100× oil objective lens (Olympus Plan Apo 100× NA 1.45) and an ANDOR iXon DU-897D-500 camera. Images were taken using Andor iQ2 software (Andor Oxford instruments). All 3D immunofluorescence images were drawn using Imaris software.

SEM images of NE-4C mouse NSCs were derived from samples cultured in vitro for 5 days after differentiation induction. The SEM images of hippocampal neurons were cultured for 7 DIV to 13 DIV. These samples were washed with DPBS and then fixed with 4% paraformaldehyde in DPBS at 4 °C for 20 min. Progressive and gradual dehydration steps were carried out by rinsing the samples with increasing ethanol solutions (0%, 5%, 10%, 20%, 30%, 50%, 70%, 90%, 95%, and 100% in deionized water). The samples were then dried under supercritical conditions and sputtered with gold before SEM investigation.

Statistical Analysis: To measure the influence of the spacings between micropillars on axons and dendrites, the neurite orientation angle, length and branch of NE-4C cells were calculated by ImageJ and Origin software. In particular, the direction of the axons and dendrites was measured as the angle (0–180°) consisting of neurites and axes parallel to the proximal axis. The lengths of axons and dendrites were measured by manually tracking axons and dendrites from soma to neurite terminal using ImageJ plug-in "Neuron J."[37] To demonstrate the universality and biocompatibility of materials and structures, immunofluorescence staining was used to observe the effect of in vitro culture time on the neurite orientation angle. The orientation angle of each neurite was measured as the angle between the neurite vector and proximal axis of the image plane. The number of cells near a specific angle value was expressed as a percentage of cells.

Quantitative analysis was performed by manually outlining the contour of every identifiable cell using ImageJ software. All statistical analyses were performed using Origin software with a sample size of $n \geq 3$. All results are expressed as the mean ± standard deviation (SD). Statistical analyses were performed via the one-way ANOVA for different groups. Statistical significance was defined as *$p < 0.05$, **$p < 0.01$, and ***$p < 0.001$.

Recording of Ca^{2+} Activity: The spontaneous activity of neuronal networks on micropillar scaffolds was investigated by functional Ca^{2+} imaging. Such images have been widely used to monitor neuronal activity both in vitro and in vivo. Ca^{2+} influx was generated by neuronal action potentials; therefore, Ca^{2+} indicators can be used to monitor the neuronal activity. At 13 days of in vitro culture, the cell culture was incubated in a mixed solution of Fluo-8 (TefLabs) and F127 (Invitrogen P6867) at 37 °C for 15 min in an external cellular solution (ECS) containing (in mM) 150 NaCl, 3 KCl, 3 CaCl$_2$, 2 MgCl$_2$, 10 HEPES, and 5 D-glucose and then washed with ECS twice.[34] The substrate was then removed from the incubator and placed on a microscope stage for imaging. For each experiment, the calcium imaging area was recorded through its original coordinate in the Andor Revolution xD 99S106 LE Flat Top stage, and then image stacks (512 × 512 pixels, 0.267 or 0.16 μm per pixel) were collected. All images were obtained in culture external medium with 20×10^{-6} M bicuculline methiodode (Tocris 2503) at room temperature at a rate of ≈33 frames per second ($\Delta t = 30$ ms). Spontaneous cellular activity was typically recorded for 1 min, and data were analyzed by ImageJ and Origin software.

Live Ca^{2+} imaging stacks were filtered with a $\sigma = (0, 0, 2)$ Gaussian function to reduce the noise in the z-axis. To minimize the effect from calcium imaging fluctuation to the fluorescent baseline, the median fluorescent intensity was chosen as F_0 and then calculated the $\Delta F/F$ of every pixel in the imaging stack to generate a new stack that represented the $\Delta F/F$ of the original stack. Then, the maximum and the minimum intensity projection was performed to the $\Delta F/F$ stack and the two projection images to create a new image named the MIP image were summarized. To further quantify the observations of Ca^{2+} activity, the spatial distribution of $\Delta F/F$ of neurons in the micropillar samples was analyzed. F_0 was the average fluorescence intensity of the selected region from an initial baseline period without activity, F was the fluorescence value of the selected region, and ΔF was the change in the fluorescence intensity ($\Delta F = F - F_0$).[38] In the neuronal network formed by neurons grown on micropillar scaffolds with various spacings and heights, the spontaneous Ca^{2+} activity of four representative sites was recorded.

Live Cell Imaging: Hippocampal neurons were imaged using a Leica DMi8 Auto microscope through a 20× lens at 2–5 DIV in NeuroBasal medium (Thermo Fisher) supplemented with 1× Glutamax (Thermo Fisher) and 1× B27 (Thermo Fisher) under 5% CO$_2$, and 37 °C conditions. Over 4–10 h, a phase contrast image was captured every 5 or 10 min.

Supporting Information

Supporting Information is available from the Wiley Online Library or from the author.

Acknowledgements

Conflict of Interest

The authors declare no conflict of interest.

Data Availability Statement

Research data are not shared.

Keywords

[1] M. Ikram, R. Ullah, A. Khan, M. O. Kim, *Cells* **2020**, *9*, 1464.
[2] H. Xia, X. Li, W. Gao, X. Fu, R. H. Fang, L. Zhang, K. Zhang, *Nat. Rev. Mater.* **2018**, *3*, 174.

**ADVANCED
SCIENCE NEWS**

www.advancedsciencenews.com

**ADVANCED
HEALTHCARE
MATERIALS**

www.advhealthmat.de

[3] A. Farrukh, S. Zhao, A. del Campo, *Front. Mater.* **2018**, *5*, 62.

[4] X. Jiang, H. Q. Cao, L. Y. Shi, S. Y. Ng, L. W. Stanton, S. Y. Chew, *Acta Biomater.* **2012**, *8*, 1290.

[5] S. W. Moore, M. P. Sheetz, *Dev. Neurobiol.* **2011**, *71*, 1090.

[6] M. H. Kim, M. Park, K. Kang, I. S. Choi, *Biomater. Sci.* **2014**, *2*, 148.

[7] V. Melissinaki, A. A. Gill, I. Ortega, M. Vamvakaki, A. Ranella, J. W. Haycock, C. Fotakis, M. Farsari, F. Claeyssens, *Biofabrication* **2011**, *3*, 045005.

[8] C. Simitzi, P. Efstathopoulos, A. Kourgiantaki, A. Ranella, I. Charalampopoulos, C. Fotakis, I. Athanassakis, E. Stratakis, A. Gravanis, *Biomaterials* **2015**, *67*, 115.

[9] T. Repić, K. Madirazza, E. Bektur, D. Sapunar, *Sci. Rep.* **2016**, *6*, 1.

[10] D. Y. Fozdar, J. Y. Lee, C. E. Schmidt, *Biofabrication* **2010**, *2*, 035005.

[11] G. Li, X. Zhao, L. Zhang, J. Yang, W. Cui, Y. Yang, H. Zhang, *Appl. Mater. Today* **2020**, *18*, 100468.

[12] M. Park, E. Oh, J. Seo, M.-H. Kim, H. Cho, J. Y. Choi, H. Lee, I. S. Choi, *Small* **2016**, *12*, 1148.

[13] C. Simitzi, A. Ranella, E. Stratakis, *Acta Biomater.* **2017**, *51*, 21.

[14] J. Seo, J. Kim, S. Joo, Y. ChoiK. KangW. K. Cho, I. S. Choi, *Small* **2018**, *14*, 1801763.

[15] O. Urwyler, A. Izadifar, S. Vandenbogaerde, S. Sachse, A. Misbaer, D. Schmucker, *Science* **2019**, *364*, 6439.

[16] H. M. Rostam, S. Singh, N. E. Vrana, M. R. Alexander, A. M. Ghaemmaghami, *Biomater. Sci.* **2015**, *3*, 424.

[17] S. Ankam, M. Suryana, L. Y. Chan, A. A. K. Moe, B. K. K. Teo, J. B. K. Law, M. P. Sheetz, H. Y. Low, E. K. F. Yim, *Acta Biomater.* **2013**, *9*, 4535.

[18] F. Klein, B. Richter, T. Striebel, C. M. Franz, G. v. Freymann, M. Wegener, M. Bastmeyer, *Adv. Mater.* **2011**, *23*, 1341.

[19] Z. Wang, Z. Du, J. K. Y. Chan, S. H. Teoh, E. S. Thian, M. Hong, *ACS Biomater. Sci. Eng.* **2015**, *1*, 1239.

[20] M. Marcus, K. Baranes, M. Park, I. S. Choi, K. Kang, O. Shefi, *Adv. Healthcare Mater.* **2017**, *6*, 1700267.

[21] S. J. Lee, T. Esworthy, S. Stake, S. Miao, Y. Y. Zuo, B. T. Harris, L. G. Zhang, *Adv. Biosyst.* **2018**, *2*, 1700213.

[22] P. Soman, B. T. D. Tobe, J. W. Lee, A. M. Winquist, I. Singec, K. S. Vecchio, E. Y. Snyder, S. C. Chen, *Biomed. Microdevices* **2012**, *14*, 829.

[23] K. Baranes, D. Kollmar, N. Chejanovsky, A. Sharoni, O. Shefi, *J. Mol. Histol.* **2012**, *43*, 437.

[24] D. Y. Fozdar, J. Y. Lee, C. E. Schmidt, S. C. Chen, *Int. J. Nanomed.* **2011**, *6*, 45.

[25] C. Peter, B. Stephen, C. Patricia, *J. Cell Sci.* **1993**, *105*, 203.

[26] S. B. Yu, J. Baek, M. Choi, Y. Oh, H. R. Lee, S. J. Yu, E. Lee, J.-W. Sohn, S. G. Im, S. Jon, *ACS Nano* **2016**, *10*, 9909.

[27] H. Dana, Y. Sun, B. Mohar, B. K. Hulse, A. M. Kerlin, J. P. Hasseman, G. Tsegaye, A. Tsang, A. Wong, R. Patel, J. J. Macklin, Y. Chen, A. Konnerth, V. Jayaraman, L. L. Looger, E. R. Schreiter, K. Svoboda, D. S. Kim, *Nat. Methods* **2019**, *16*, 649.

[28] Y. Zhang, Y. Li, Y. Hu, X. Zhu, Y. Huang, Z. Zhang, S. Rao, Z. Hu, W. Qiu, Y. Wang, *Adv. Mater.* **2018**, *30*, 1803072.

[29] A. Koitmäe, M. Müller, C. S. Bausch, J. Harberts, W. Hansen, G. Loers, R. H. Blick, *Langmuir* **2018**, *34*, 1528.

[30] D. E. Koser, A. J. Thompson, S. K. Foster, A. Dwivedy, E. K. Pillai, G. K. Sheridan, H. Svoboda, M. Viana, L. F. Costa, J. Guck, C. E. Holt, K. Franze, *Nat. Neurosci.* **2016**, *19*, 1592.

[31] S. Weigel, T. Osterwalder, U. Tobler, L. Yao, M. Wiesli, T. Lehnert, A. Pandit, A. J. P. o. Bruinink, *PLoS One* **2012**, *7*, 50714.

[32] S. Q. Chen, Q. Cai, Y. Y. Shen, X. Y. Cai, H. Y. Lei, *Int. J. Dev. Neurosci.* **2014**, *38*, 74.

[33] A. Marino, G. Ciofani, C. Filippeschi, M. Pellegrino, M. Pellegrini, P. Orsini, M. Pasqualetti, V. Mattoli, B. Mazzolai, *ACS Appl. Mater. Interfaces* **2013**, *5*, 13012.

[34] A. Odawara, M. Gotoh, I. Suzuki, *Lab Chip* **2013**, *13*, 2040.

[35] C. L. Tao, Y. T. Liu, R. Sun, B. Zhang, L. Qi, S. Shivakoti, C. L. Tian, P. Zhang, P. M. Lau, Z. H. Zhou, G. Q. Bi, *J. Neurosci.* **2018**, *38*, 1493.

[36] Z. X. Fu, X. Tan, H. Fang, P. M. Lau, X. Wang, H. Cheng, G. Q. Bi, *Nat. Commun.* **2017**, *8*, 1.

[37] E. Meijering, M. Jacob, J.-C. F. Sarria, P. Steiner, H. Hirling, M. Unser, *Cytometry, Part A* **2004**, *58*, 167.

[38] V. Gautam, S. Naureen, N. Shahid, Q. Gao, Y. Wang, D. Nisbet, C. Jagadish, V. R. Daria, *Nano Lett.* **2017**, *17*, 3369.